PROCEEDINGS OF SCIENCE

New constraints on nucleon structure from LHCb

Sara Sellam[a,*]

[a] ***on behalf of the LHCb collaboration***
IGFAE (Universidade de Santaigo de Compostela),
Rúa de Xoaquín Díaz de Rábago, Santiago de Compostela, Spain

E-mail: sara.sellam@usc.es

The forward geometry of the LHCb detector provides unprecedented access to both the very high and very low regions of Bjorken x inside the nucleon. With full particle identification and a fast data acquisition (DAQ), LHCb is able to fully reconstruct plentiful charged particles and π^0 mesons, as well as relatively rare probes such as Z bosons and heavy quarks, providing a unique set of constraints on nucleon structure functions. This talk will discuss recent LHCb measurements sensitive to intrinsic charm within the proton, modification of parton distribution functions inside the nucleus, and show the impact of recent LHCb measurements that dramatically reduce the nuclear parton distribution function (nPDF) uncertainties at low x.

HardProbes2023
26-31 March 2023
Aschaffenburg, Germany

*Speaker

PoS(HardProbes2023)044

1. Introduction

The LHCb experiment [1] is a forward detector with excellent vertex reconstruction, particle tracking, and identification [2], it has made significant contributions to the field of heavy ion physics in recent years. Recent LHCb-D measurements [3] have significantly constrained the nuclear parton distribution functions (nPDFs) down to $x \sim 10^{-5}$ [4]. In these proceedings, we present three recent LHCb results that provide valuable insights for refining and improving our understanding of the nPDFs.

2. Neutral pion production in pPb at $\sqrt{s_{\rm NN}} = 8.16$ TeV

Neutral pion production plays a crucial role in probing the behavior of nuclear matter in heavy ion collisions. In particular, pPb collisions provide a unique opportunity to study the effects of cold nuclear matter (CNM) on the initial state of bound nucleons within the colliding nucleus. The CNM effects that include the modification of the initial parton density compared to that of the proton are encoded into the nuclear parton distribution functions (nPDFs) [5], which are determined through fits to experimental data, although they remain poorly constrained for partons with momentum fraction x smaller than approximately 10^{-4}. Therefore, studying neutral-pion production in pPb collisions can help refine our understanding of nPDF in the low-x region. The LHCb experiment has recently measured the nuclear modification factor of π^0 meson at $\sqrt{s_{\rm NN}} = 8.16$ TeV [6]. The nuclear modification factor is given by

$$R_{p\rm Pb} = \frac{1}{A}\frac{d\sigma_{p\rm Pb}/dp_{\rm T}}{d\sigma_{pp}/dp_{\rm T}}, \tag{1}$$

where A=208 is the atomic mass number of the lead nucleus and $d\sigma_{p\rm Pb}/dp_{\rm T}$ and $d\sigma_{pp}/dp_{\rm T}$ are the π^0 differential production cross sections in pPb and proton-proton (pp) collisions, respectively. The cross-section in pp collisions at $\sqrt{s_{\rm NN}} = 8.16$ TeV is estimated by interpolating between the measured pp cross-sections at $\sqrt{s_{\rm NN}} = 5$ TeV and $\sqrt{s_{\rm NN}} = 13$ TeV, and it represents the largest source of uncertainties. The nuclear modification factor in figure 1 shows a Cronin-like enhancement larger than predicted by the pQCD calculations at backward rapidities. In the forward region, the data are much smaller than the nPDF uncertainties, indicating that this measurement can provide powerful constraints on nPDF at low x. The measurement is also compared to the $R_{p\rm Pb}$ measured by the LHCb experiment in pPb collisions at $\sqrt{s_{\rm NN}} = 5$ TeV [9], in the forward pseudorapidity at the center-of-mass frame (CMS) ($2.5 < \eta_{\rm CMS} < 3.5$) region π^0 measurement agrees with the charged-particles measurement, unlike the backward rapidities ($-4 < \eta_{\rm CMS} < -3$) where the enhancement observed in π^0 is larger than the one in charged particles, which may indicate a mass ordering effect.

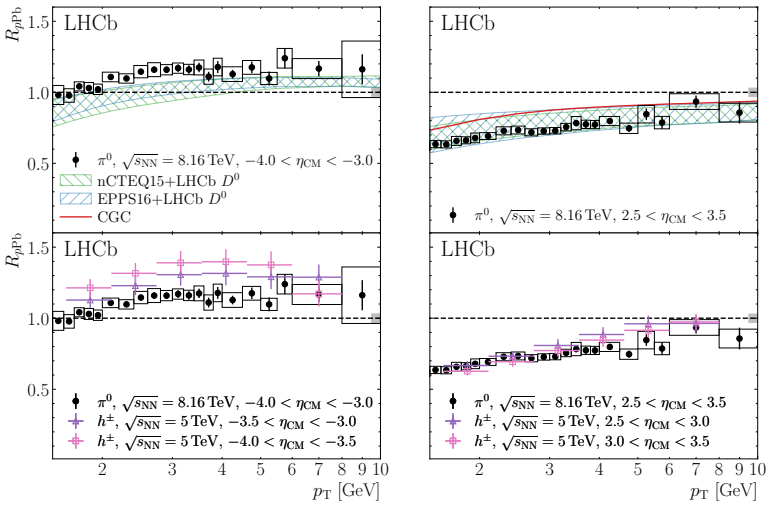

Figure 1: Measured π^0 nuclear modification factor in the (left) backward and (right) forward $\eta_{\rm CM}$ regions. The statistical uncertainties are represented by error bars, while open boxes represent the systematic uncertainties. The results are compared to (top) theoretical predictions [4, 7, 8] and (bottom) to charged-particle data from Ref. [9]. The hatched regions show the nPDF uncertainties of the pQCD calculations.

3. Measurement of Z boson production cross section in pPb collisions at $\sqrt{s_{\rm NN}} = 8.16$ TeV

The production of inclusive Z-boson is an important process to study the initial state effects and constraining nuclear parton distribution functions. The LHCb experiment has measured for the first time [10] the inclusive $Z \to \mu^+\mu^-$ production in pPb collisions at a nucleon-nucleon center-of-mass energy of $\sqrt{s_{\rm NN}} = 8.16$ TeV, defined as:

$$R^{fw}_{p\rm Pb} = k^{fw}_{p\rm Pb}(x)\frac{1}{A}\frac{d\sigma_{(p\rm Pb,1.53<y^*_\mu<4.03)}/dx}{d\sigma_{(pp,2.0<y^*_\mu<4.5)}/dx}, \tag{2}$$

$$R^{bw}_{p\rm Pb} = k^{bw}_{p\rm Pb}(x)\frac{1}{A}\frac{d\sigma_{(p\rm Pb,-4.97<y^*_\mu<-2.47)}/dx}{d\sigma_{(pp,-4.5<y^*_\mu<-2.0)}/dx}, \tag{3}$$

Where A = 208 is the mass number of the Pb, y^*_μ is the μ rapidity in the CMS frame, x is either the Z rapidity in the CMS frame ($y^*_{\rm Z}$), $p^{\rm Z}_{\rm T}$ or the angle ϕ^*. $k(x)$ is a factor to correct for the different y^*_μ acceptance between pPb and pp collisions and can be calculated using PowHegBox [11–14] with the proton PDF set CTEQ6.1 [15].

$$k^{fw}_{p\rm Pb}(x) = \frac{d\sigma'_{(pp,2.0<y^*_\mu<4.5)}/dx}{d\sigma'_{(pp,1.53<y^*_\mu<4.03)}/dx} \tag{4}$$

$$k^{bw}_{p\rm Pb}(x) = \frac{d\sigma'_{(pp,-4.5<y^*_\mu<-2.0)}/dx}{d\sigma'_{(pp,-4.97<y^*_\mu<-2.47)}/dx} \tag{5}$$

The prime symbol (σ') in the equation indicates that the corresponding cross-section is calculated theoretically instead of from data measurements.

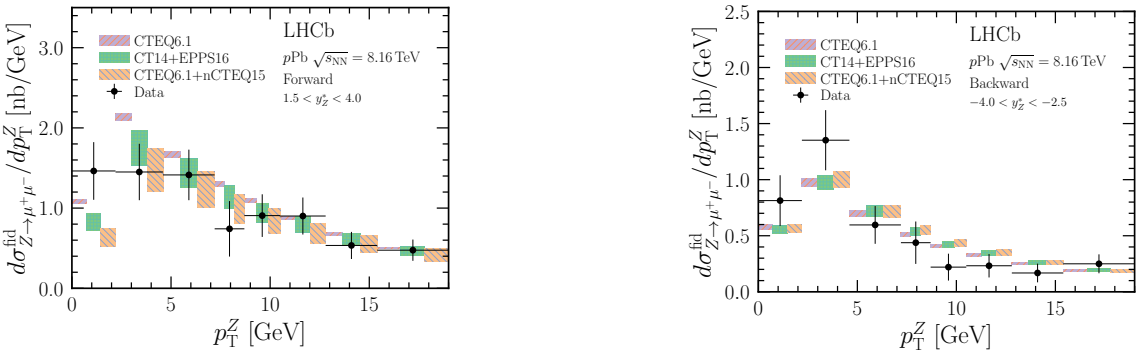

Figure 2: The measured differential fiducial cross-section as a function of $p_{\mathrm{T}}^{\mathrm{Z}}$ in the forward region (left) and backward region (right). The theoretical predictions are calculated using PowhegBox with CTEQ6.1, EPPS16 [5, 16], and nCTEQ15 (n)PDF sets [17].

The cross-section is shown in figure 2 as a function of $p_{\mathrm{T}}^{\mathrm{Z}}$ at low transverse momentum with finer intervals to aid theoretical transverse momentum dependent studies.

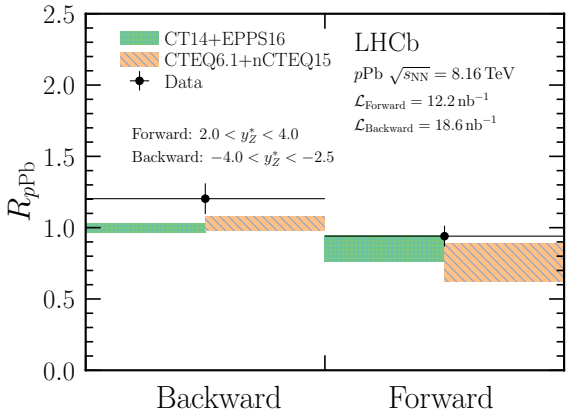

Figure 3: Measurements of the nuclear modification factor compared to the PowhegBox predictions using the EPPS16 and nCTEQ15 (n)PDF sets.

The measured nuclear modification factor figure 3 is compatible with theoretical predictions from EPPS16 and nCTEQ15 nPDFs.

4. Study of Z bosons produced in association with charm in the forward region of pp collision at $\sqrt{s_{\mathrm{NN}}} = 13$ TeV

To investigate the internal structure of the proton, LHCb has measured the production of Z bosons in association with charm quarks in the forward region of proton-proton collisions at $\sqrt{s_{\mathrm{NN}}} = 13$ TeV [22]. The ratio of production cross-section $\mathcal{R}_j^c \equiv \sigma(\mathrm{Z}c)/\sigma(\mathrm{Z}j)$ where $\mathrm{Z}c$ refers to events containing a Z boson and c jets, $\mathrm{Z}j$ refers to events containing a Z boson and any type of jet, was chosen because it is less sensitive than $\sigma(\mathrm{Z}c)$ to experimental and theoretical uncertainties. The Z bosons are reconstructed using the $Z \to \mu^+\mu^-$ decay, the c jets are identified using c-tagging algorithm [1] which looks for a displaced-vertex (DV) signature inside the jet cone. After identifying

jets with DVs, the algorithm uses a two-dimensional fit to the number of tracks in the DV, $N_{\text{trk}}(\text{DV})$, and the corrected mass, $m_{\text{cor}}(\text{DV}) \equiv \sqrt{m(\text{DV})^2 + [p(\text{DV})\sin\theta]^2} + p(\text{DV})\sin\theta$, where θ is the angle between the momentum and the flight direction of the DV, to determine the composition of the tagged sample.

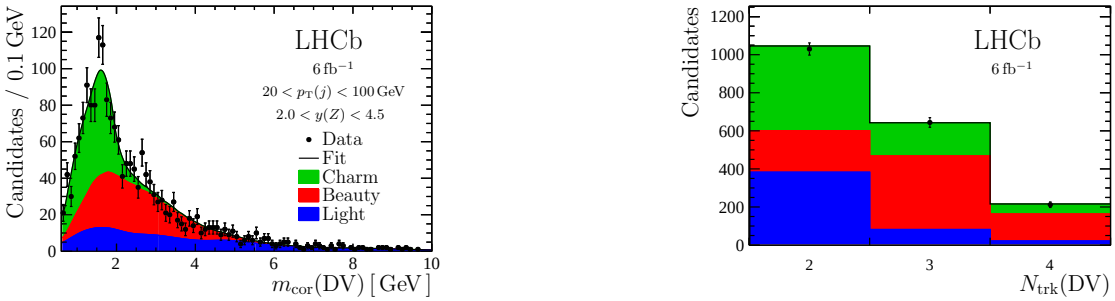

Figure 4: The distributions of (left) $m_{\text{cor}}(\text{DV})$ and (right) $N_{\text{trk}}(\text{DV})$ for all candidates tagged with DV in the Zj data sample reconstructed in the fiducial region are presented. The projections of the fit results are superimposed on the distributions. The predictions are offset in each interval to improve visibility.

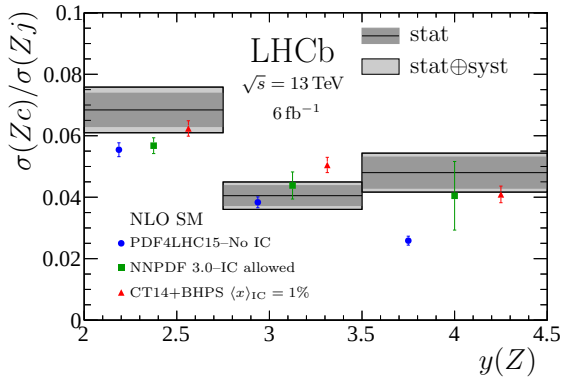

Figure 5: $\mathcal{R}_j^c$ distribution represented as gray bands for three intervals of forward Z rapidity, compared to NLO SM predictions without intrinsic charm (IC) in blue [19], with the charm PDF shape allowed to vary in green [20] and with IC as predicted by BHPS with a mean momentum fraction of 1%. [21] in red.

The measured $\mathcal{R}_j^c$ distribution in intervals of the pseudo-rapidity of the Z (y(Z)) is shown in figure 5. The ratio is consistent with both the no intrinsic charm (IC) and IC hypotheses in the first two y(Z) bins. As for the most forward bin, a large enhancement is observed consistent with IC PDF shape predicted by BHPS [21]. Incorporating the result into global analysis should strongly constrain the large-x charm PDF, both in size and in shape.

5. Perspectives

LHCb experiment has obtained a plethora of interesting results in the field of heavy ion physics that considerably reduced the nPDFs uncertainties. It is expected to make a significant contribution during the upcoming LHC runs, taking advantage of the ongoing detector upgrade and the new fixed target program.

References

[1] A. A. Alves, Jr. *et al.* [LHCb], JINST **3** (2008), S08005

[2] R. Aaij *et al.* [LHCb], Int. J. Mod. Phys. A **30** (2015) no.07, 1530022

[3] R. Aaij *et al.* [LHCb], JHEP **10** (2017), 090

[4] K. J. Eskola, I. Helenius, P. Paakkinen and H. Paukkunen, JHEP **05** (2020), 037

[5] K. J. Eskola, P. Paakkinen, H. Paukkunen and C. A. Salgado, Eur. Phys. J. C **77** (2017) no.3, 163

[6] A. A. Alves, Jr. *et al.*[LHCb], arXiv:2204.10608 [nucl-ex]

[7] I. Helenius, K. J. Eskola and H. Paukkunen, JHEP **09** (2014), 138

[8] T. Lappi and H. Mäntysaari, Phys. Rev. D **88** (2013), 114020

[9] R. Aaij *et al.* [LHCb], Phys. Rev. Lett. **128** (2022) no.14, 142004

[10] R. Aaij *et al.* [LHCb], JHEP **06** (2023), 022

[11] P. Nason, JHEP **11** (2004), 040

[12] S. Frixione, P. Nason and C. Oleari, JHEP **11** (2007), 070

[13] S. Alioli, P. Nason, C. Oleari and E. Re, JHEP **06** (2010), 043

[14] S. Alioli, P. Nason, C. Oleari and E. Re, JHEP **07** (2008), 060

[15] D. Stump, J. Huston, J. Pumplin, W. K. Tung, H. L. Lai, S. Kuhlmann and J. F. Owens, JHEP **10** (2003), 046

[16] S. Dulat, T. J. Hou, J. Gao, M. Guzzi, J. Huston, P. Nadolsky, J. Pumplin, C. Schmidt, D. Stump and C. P. Yuan, Phys. Rev. D **93** (2016) no.3, 033006

[17] K. Kovarik, A. Kusina, T. Jezo, D. B. Clark, C. Keppel, F. Lyonnet, J. G. Morfin, F. I. Olness, J. F. Owens and I. Schienbein, *et al.* Phys. Rev. D **93** (2016) no.8, 085037

[18] T. Boettcher, P. Ilten and M. Williams, Phys. Rev. D **93** (2016) no.7, 074008

[19] J. Butterworth, S. Carrazza, A. Cooper-Sarkar, A. De Roeck, J. Feltesse, S. Forte, J. Gao, S. Glazov, J. Huston and Z. Kassabov, *et al.* J. Phys. G **43** (2016), 023001

[20] R. D. Ball *et al.* [NNPDF], Eur. Phys. J. C **76** (2016) no.11, 647

[21] T. J. Hou, S. Dulat, J. Gao, M. Guzzi, J. Huston, P. Nadolsky, C. Schmidt, J. Winter, K. Xie and C. P. Yuan, JHEP **02** (2018), 059

[22] R. Aaij *et al.* [LHCb], Phys. Rev. Lett. **128** (2022) no.8, 082001